

# The application of the self-adaptive tracking method to the sinusoidal phase modulating interferometry

GUOTIAN HE<sup>1, 2, 4\*</sup>, YUANGANG LU<sup>3</sup>, CHANGRONG LIAO<sup>2</sup>, ZHI ZENG<sup>1</sup>

<sup>1</sup>Chongqing Optical Engineering Key Laboratory, College of Physics and Information Technology, Chongqing Normal University, Chongqing 400030, China

<sup>2</sup>Chongqing University College of Optoelectronic Engineering, Chongqing 400047, China

<sup>3</sup>Institute of Optical Communication Engineering, School of Engineering and Management, Nanjing University, Nanjing 210093, China

<sup>4</sup>Shanghai Institute of Optics and Fine Mechanics, Chinese Academy of Sciences, Shanghai 201800, China

\*Corresponding author: slhgt@mail.siom.ac.cn

In this paper, we analyze theoretically the accuracy of the surface profile measurement in a sinusoidal phase modulating interferometer, derive the relative error formula, and investigate the influence of spectral leakage on the measurement accuracy. The theoretical results show that when the offset of sampling frequency from its theoretical ideal is outside the range of  $-0.188\%$  to  $+0.075\%$ , the spectrum leakage results in an relative error greater than  $\lambda/320$  nm, and thus the spectral leakage is not negligible. In order to eliminate the influence of the spectral leakage, a self-adaptive tracking method is proposed. The tracking method can adjust automatically the sampling signal frequency in such a way that the sampling signal frequency is an integer multiple of the modulating signal frequency. The simulation and experimental results show that the problem of the spectrum leakage can be solved with the proposed technique, and therefore the measurement accuracy and reliability of the SPM interferometer are enhanced.

Keywords: sinusoidal phase modulation, surface profile measurement, spectral leakage, self-adaptive tracking method, DFT analysis.

## 1. Introduction

In 1986, SASAKI and OKAZAKI [1] proposed a new sinusoidal phase modulating (SPM) interferometer. This technique introduces a sinusoidal vibrating piezoelectric transducer (PZT) in a Michelson interferometer to modulate the phase of the reference beam. In the SPM interferometry, there is a modulation component in the phase of the interference signal when compared with that of the traditional interference signal.

After demodulation to the interference signal with Fourier analysis method, the phase corresponding to the measured object can be extracted from the interference signal, and the physical quantities such as distance and surface height can be obtained. This interferometry has the advantages of high accuracy, high resolution and simple modulation, and is widely used in the measurement of surface profile, displacement, vibration, *etc.* [2–9].

In SPM interferometry, the interference signal is periodic. The sampling clock signal must synchronize with the interference signal during the signal sampling period. If the sampling frequency changes, arising from the disturbance of the interference signal or sampling clock signal, the Fourier transformation of the sampling sequence shows spectrum leakage and cut-off error [10]. The influence of the spectrum leakage on the measured results is not negligible because it causes the measurement accuracy of the SPM interferometer to deteriorate. At present, there exist two methods to solve the problem of the spectrum leakage. One is to increase the number of sampling points or enhance the sampling frequency, the other is to introduce window function or interpolation method [11–13]. However, these methods take a long time to process the data, and the improvement of the spectrum leakage is very limited. Therefore, these methods are not suitable for the SPM interferometric measurement.

In this paper, we analyze theoretically the spectrum leakage in the SPM interferometry, illustrate the reasons of the spectrum leakage, derive the error formula, and simulate the influence of spectral leakage on measurement accuracy. The simulated result verifies the correctness of the theoretical analysis. And a self-adaptive tracking method is proposed to solve the problem arising from spectrum leakage in SPM interferometry. The tracking method enhances greatly the measurement accuracy of the SPM interferometry.

## 2. SPM interferometer signal and its sampling

Figure 1 shows the experimental setup of the SPM interferometer. Light from a He-Ne laser is split into object and reference beams by the beam splitter (BS). The two beams are reflected by the object and reference mirror (M), respectively, and interfered to form the interference signal, and this signal is captured with a CCD image sensor. The reference beam is phase modulated with a sinusoidal vibrating mirror

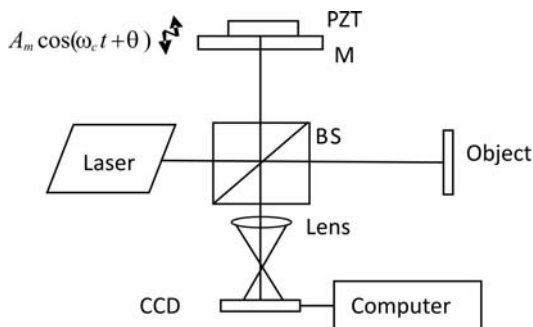


Fig. 1. Sinusoidal phase modulating interferometer.

attached to a piezoelectric transducer (PZT). The modulation signal driving the PZT is given by [14]

$$A(t) = A_m \cos(\omega_c t + \theta) \quad (1)$$

where  $A_m$ ,  $\omega_c$  and  $\theta$  are the amplitude, angular frequency and initial phase of the modulation signal, respectively. The AC component of the interference signal accepted by CCD image sensor is given by [15]

$$s(x, y, t) = s_0(x, y) \cos[z \cos(\omega_c t + \theta) + \alpha(x, y)] \quad (2)$$

where  $z = 4\pi A_m / \lambda$  is the modulation depth,  $s_0(x, y)$  is the amplitude of the AC component at point  $(x, y)$  of the measured object, and  $\alpha(x, y)$  is the measured phase at point  $(x, y)$  at time  $t$ .

By a series expansion, Eq. (2) can be given by

$$s(x, y, t) = \sum_{k=0}^m A_k \exp\left\{j\left[k(\omega_c t + \theta) + \alpha(x, y)\right]\right\} \quad -\infty < t < \infty \quad (3)$$

where  $m$  is the maximum harmonic order,  $A_k$  is the amplitude corresponding to the  $k$ -th harmonic component. Let the sampling frequency of signal  $s(x, y, t)$  be  $f_s$ , and we can get the discrete signal  $s(x, y, n)$

$$\begin{aligned} s(x, y, n) &= s(x, y, t) \Big|_{t=nT_s} = \\ &= \sum_{k=0}^m A_k \exp\left\{j\left[k\theta + \alpha(x, y)\right]\right\} \exp\left[jkn\omega_c T_s\right] = \\ &= \sum_{k=0}^m A_k \exp\left\{j\left[k\theta + \alpha(x, y)\right]\right\} \exp\left[\frac{j2\pi knT_s}{T_c}\right] \quad -\infty < n < \infty \end{aligned} \quad (4)$$

where the sampling period  $T_s = 1/f_s$ ,  $T_c = 1/f_c = 2\pi/\omega_c$ , and  $n$  is the sampling sequence number. The total  $N$  points are sampled during interference signal sampling, and  $N \geq 2m$ . We assume that  $N$  is equal to  $T_s/T_c$  (exactly an integer value) which means signal  $s(n)$  is truncated by rectangular window function. The rectangular window function is given by

$$d(n) = \begin{cases} 1 & 0 \leq n \leq N \\ 0 & n < 0, n > N \end{cases} \quad (5)$$

After being multiplied by rectangular window function, the sequence signal  $s(x, y, n)$  can be expressed as

$$s_d(x, y, n) = s(x, y, n) d(n) \quad (6)$$

If  $N > 2m$ , the discrete Fourier transform (DFT) of Eq. (6) is given by

$$S_d(x, y, \omega) = \text{DFT} \left[ s(x, y, n)d(n) \right] = \frac{1}{2\pi} S(x, y, \omega) * D(\omega) \quad (7)$$

where the  $*$  is the convolution sign. Expanding the above equation, we have

$$\begin{aligned} S_d(x, y, \omega) = & \\ = & F \left\{ \cos [\alpha(x, y)] \right\} \left\{ J_0(z) + J_1(z) \left[ \delta(\omega - \omega_c) \exp(j\theta) + \delta(\omega - \omega_c) \exp(-j\theta) \right] + \dots \right\} + \\ & - F \left\{ \sin [\alpha(x, y)] \right\} \left\{ -J_2(z) \left[ \delta(\omega - 2\omega_c) \exp(j2\theta) + \delta(\omega - 2\omega_c) \exp(-j2\theta) \right] - \dots \right\} \end{aligned} \quad (8)$$

$J_m(z)$  is the  $m$ -th order Bessel function,  $\delta$  is the Dirac delta function, and  $F\{\}$  is Fourier transformation operator.

The phase difference of two adjacent points in the frequency domain can be expressed as

$$\Delta \Phi = \frac{2\pi}{N} \quad (9)$$

When the frequency of the modulated signal is constant,  $\Delta \Phi$  is also constant according to Eq. (9). Therefore, if the signal is sampled uniformly in time domain, the phase is the same in the corresponding frequency domain [16]. When  $\delta(\Delta\omega) = 1$ , the frequency of the interference signal has no fluctuation in Eq. (8), which means that the 1st, 2nd and 3rd order spectrum ( $S_1$ – $S_3$ ) have no frequency leakage at  $\omega = \omega_c$ ,  $\omega = 2\omega_c$ ,  $\omega = 3\omega_c$ , when  $|\omega| > \omega_c/2$ ,  $F\{\cos[\alpha(x, y)]\} = 0$ ,  $F\{\sin[\alpha(x, y)]\} = 0$  [14].

When  $|\omega| < \omega_c/2$  [14], the 1st, 2nd, and 3rd order spectrum of the modulated signal can be given by:

$$S_1(x, y, \omega) = -J_1(z) F \left\{ \sin [\alpha(x, y)] \right\} \quad (10)$$

$$S_2(x, y, \omega) = -J_2(z) F \left\{ \cos [\alpha(x, y)] \right\} \quad (11)$$

$$S_3(x, y, \omega) = J_3(z) F \left\{ \sin [\alpha(x, y)] \right\} \quad (12)$$

According to Eqs. (10)–(12),  $z$  and  $\theta$  can be obtained, and following relation is obtained [14]:

$$\tan [\alpha(x, y)] = \left| \frac{S_1(x, y, \omega)/J_1(z)}{S_2(x, y, \omega)/J_2(z)} \right| \quad (13)$$

Then the surface profile of the measured object can be given by

$$r(x, y) = \frac{\lambda \alpha(x, y)}{4\pi} \quad (14)$$

Therefore, according to Eqs.(10) and (12), there is no error due to frequency leakage at the measured surface profile  $r(x, y)$ .

If the interference signal is obtained by sampling non-uniformly, the modulated frequency changes minimally near the normal frequency. Therefore, the change in modulated frequency is negligible corresponding to the  $2\pi/N$  change of phase angle of frequency domain [16]. As well as in the case of uniform sampling, and  $\delta(\Delta\omega) \approx 1$  ( $\Delta\omega \approx 0$ ) in Eq. (8), which means that the 1st, 2nd, and 3rd order spectrum ( $S_1$ – $S_3$ ) have no frequency leakage at  $\omega = \omega_c$ ,  $\omega = 2\omega_c$ ,  $\omega = 3\omega_c$ .

### 3. Spectrum leakage of the SPM interferometer signal

Next, we discuss the reasons of the spectrum leakage of the SPM interferometer signal. During the sampling process, the sampling frequency  $f_s$  and sampling point number  $N$  are kept constant, while the frequency of the measured interference signal may fluctuate due to the fluctuations of the laser frequency. Let the real frequency of the modulated signal be  $f'_c$ . We define

$$\varepsilon = \frac{f'_c}{f_c} = \frac{\omega}{\omega_c} = 1 + \Delta\varepsilon \quad (15)$$

According to Eq. (8), we have

$$S'_1(x, y, \omega = \varepsilon\omega_c) = -J_1(z) \left[ \delta(\varepsilon\omega_c - \omega_c) \exp(j\theta) + \delta(\varepsilon\omega_c - \omega_c) \exp(-j\theta) \right] \times \\ \times F \left\{ \sin \left[ \alpha(x, y) \right] \right\} \quad (16)$$

$$S'_2(x, y, \omega = 2\varepsilon\omega_c) = -J_2(z) \left[ \delta(2\varepsilon\omega_c - 2\omega_c) \exp(j2\theta) + \delta(2\varepsilon\omega_c - 2\omega_c) \exp(-j2\theta) \right] \times \\ \times F \left\{ \cos \left[ \alpha(x, y) \right] \right\} \quad (17)$$

$$S'_3(x, y, \omega = 3\varepsilon\omega_c) = -J_3(z) \left[ \delta(3\varepsilon\omega_c - 3\omega_c) \exp(j3\theta) + \delta(3\varepsilon\omega_c - 3\omega_c) \exp(-j3\theta) \right] \times \\ \times F \left\{ \sin \left[ \alpha(x, y) \right] \right\} \quad (18)$$

When  $\varepsilon \neq 1$  and the change of modulated frequency is not negligible,  $\delta(\Delta\omega) \neq 1$  in Eqs. (16)–(18), which means that  $S'_1$ – $S'_3$  have frequency leakage at  $\omega = \omega_c$ ,  $\omega = 2\omega_c$ ,

and  $\omega = 3\omega_c$ . Each harmonic component will exhibit nonzero projection on all the elements of the basis, giving its contribution to the relevant DFT coefficients. The harmonic interference due to the spectral leakage arises, which makes the measured amplitudes of  $S'_1-S'_3$  ( $S'_1 < S_1$ ,  $S'_2 < S_2$ ,  $S'_3 < S_3$ ) less than the corresponding actual values.

In like manner, when the modulating frequency is constant but the sampling frequency is fluctuant, there also exists spectrum leakage. The interference signal of SPM is a periodic signal. When the modulating frequency changes arising from the hysteresis characteristic of the PZT and the sampling signal frequency changes minimally, which makes the integer relationship between the sampling and modulating frequency detune, the spectrum leakage occurs. This spectrum leakage will lead to the enlarged errors in measuring the modulation depth  $z$ , the initial phase of sinusoidal modulating  $\theta$ , the measured phase  $\alpha(x, y)$ , and the surface profile of the measured object  $r(x, y)$ .

#### 4. Error analysis of spectrum leakage

The modulation period of the interference signal is  $T_c$ , and the ideal sampling frequency is  $f_{s0}$  (the corresponding sampling period is  $T_{s0}$ ). When the interference signal is cut-off by rectangular window with length  $LT_{s0}$  ( $L$  is the number of cut-off periods), there exist total  $N$  discrete signal points. If the modulation frequency matches with the sampling frequency, it satisfies the relationship:

$$N = \frac{LT_c}{T_{s0}} \quad \text{or} \quad \frac{f_{s0}}{f_c} = \frac{N}{L} \quad (19)$$

So after the interference signal is sampled, the ideal sampling sequence is given by

$$\begin{aligned} s_l(n) = s(nT_{s0}) &= \sum_{k=0}^m A_m \exp[j(k\theta + \alpha)] \exp[j2\pi knf_c T_{s0}] = \\ &= \sum_{k=0}^m A_m \exp[j(k\theta + \alpha)] \exp\left[\frac{j2\pi knL}{N}\right] \end{aligned} \quad (20)$$

If the modulation frequency does not match the sampling frequency, assuming the modulation period is  $T_c$  and actual sampling frequency is  $f_s$ , it satisfies the relationship:

$$N' = \left\lceil \frac{LT_c}{T_s} \right\rceil \quad (21)$$

where  $[x]$  denotes integer part of  $x$ . After the interference signal is sampled, the actual sampling sequence is given by

$$\begin{aligned} s_s(n) &= s_a(nT_s) = \sum_{k=0}^m A_m \exp[j(k\theta + \alpha)] \exp[j2\pi knf_c T_s] = \\ &= \sum_{k=0}^m A_m \exp[j(k\theta + \alpha)] \exp\left[\frac{j2\pi knL(1 + e_{\text{err}}/T_{s0})}{N'}\right] \end{aligned} \quad (22)$$

where  $e_{\text{err}} = T_s - T_{s0}$ .

The error between ideal and actual sampling sequence, can be given by

$$\text{Error}(n) = s_l(n) - s_s(n) \quad (23)$$

Then the  $k$ -th order relative error can be expressed as

$$\text{Rerror}(n) \approx \frac{1}{2!} \left[ \frac{2\pi knLe_{\text{err}}}{N'T_{s0}} \right]^2 = \frac{1}{2!} \left[ \frac{2\pi kn e_{\text{err}} T_s}{T_c T_{s0}} \right]^2 \quad (24)$$

When the offset of the modulated frequency from its theoretical ideal is in the range from  $-2.5\%$  to  $+2.5\%$ , the relative error of the 1st spectrum component is in the range from  $0.0123\%$  to  $1.22\%$ , the relative error of the 2nd spectrum component is in the range from  $0.20\%$  to  $4.87\%$ , and the relative error of the 3rd spectrum component is in the range from  $0.11\%$  to  $10.97\%$ .

## 5. Spectrum leakage simulations

Next, we will simulate the error arising from spectrum leakage. The theoretical value of the surface profile is  $100 \text{ nm}$ , SNR  $50 \text{ dB}$  (the SNR is defined as that in ref. [17]), light wavelength  $632.8 \text{ nm}$ , modulating frequency  $400 \text{ Hz}$ , ideal sampling signal frequency  $3200 \text{ Hz}$ , the number of sampling points  $128$ . According to Eqs. (2)–(4), we get the discrete interferometer signal. After the Fourier transform to the discrete signal, the  $n$ -th ( $n = 1, 2, 3$ ) order spectrum component ( $S'_1 - S'_3$ ) with frequency leakage can be obtained when  $\delta \neq 1$ , and the simulated surface profile  $r(x, y)$  can be calculated from Eqs. (16)–(18).

We assume that the sampling frequency offset from its theoretical ideal is in the range from  $-0.375\%$  to  $+0.375\%$ , which is corresponding to the range from  $-12$  to  $12 \text{ Hz}$ . When there exists spectrum leakage, the calculated displacement  $r(x, y)$  can be obtained according to  $\alpha(x, y)$ . We can obtain the error by comparing the theoretical value with the calculated  $r(x, y)$ . The simulated spectrum leakage error is shown in

Tab. 1. The results show that when the offset of sampling frequency from its theoretical ideal is outside the range of  $-0.188\%$  to  $+0.075\%$  (corresponding to absolute error from  $-6$  to  $2.4$  Hz), the spectrum leakage results in a relative error greater than  $\lambda/320$  nm (corresponding to absolute error  $2.14$  nm), and thus the spectral leakage is not negligible.

In each different sampling frequency the displacement result is calculated 64 times each with a different degree of randomization noise. The *average displacement* is the average result of the 64 times of different calculated results. The *repeatable accuracy* of simulated displacement in Tab. 1 describes the root-mean-square (RMS) of the simulated displacement. The “error” in Tab. 1 is the difference between the “average displacement” and the theoretical displacement. When the product of the sampling frequency and the sampling length equals the integer multiple of the modulating frequency, the error is  $0.26$  nm and the spectrum leakage error is negligible. When the frequency offset is increased, the displacement error due to spectrum leakage increases quickly, and RMS error grows quickly. The theoretical results show that when the offset of sampling frequency from its theoretical ideal is outside the range of  $-0.188\%$  to  $+0.075\%$ , the spectrum leakage results in a relative error greater than  $\lambda/320$  nm, and thus the spectral leakage is not negligible.

Table 1. The errors of the simulated spectrum leakage without correction.

Modulating frequency [Hz]	Real sampling frequency [Hz]	Average displacement [nm]	Repeatable accuracy [nm]	Error [nm]
400	3212	66.68	38.16	-33.32
400	32108	68.75	78.23	-31.25
400	3209.6	73.68	63.33	-26.32
400	3208.4	71.69	40.31	-28.31
400	3207.2	74.69	5.44	-25.31
400	3206.0	102.14	3.26	2.14
400	3204.8	100.30	5.37	0.30
400	3203.6	100.07	1.88	0.07
400	3202.0	101.43	1.85	1.43
400	3201.2	100.31	0.97	0.31
400	3200	100.26	1.98	0.26
400	3198.8	102.41	4.50	2.41
400	3197.6	103.53	10.27	3.53
400	3196.4	108.22	32.25	8.22
400	3195.2	82.15	18.52	-17.85
400	3194.0	76.53	35.79	-23.47
400	3192.8	71.04	32.58	-28.96
400	3191.6	61.76	38.57	-38.24
400	3190.4	64.38	48.22	-35.62
400	3189.2	70.69	39.27	-29.31
400	3188.0	57.73	36.80	-42.27



### 6. Self-adaptive tracking method to correct the spectrum leakage

From the above description, the reason for the spectrum leakage lies in  $f_s \neq Nf_c$ . The problem of spectrum leakage can be solved only by real-time adjusting of the relationship between  $f_s$  and  $f_c$ . When the  $S(l)$  is at  $t_{k-1}$  and  $t_k$ , the frequencies are  $f_s^{k-1}$ ,  $f_s^k$  according to Eq. (7), respectively. When the sampling signal frequency is constant at the sampling interval  $2\pi/N$ ,  $f_s^{k-1} = f_s^k$ . When the sampling signal frequency fluctuates, sampling will occur at the non-uniform interval in time domain. According to the phasor theory, the phase difference  $\Delta\beta$  of the interference signal between two adjacent points is given by

$$\Delta\beta \approx 2\pi(f_s^k - f_s^{k-1})T_s^k \approx \frac{2\pi(f_s^k - f_s^{k-1})}{Nf_s^{k-1}} \tag{25}$$

Therefore the sampling signal frequency at  $k$ -th sampling point is given by

$$f_s^k = f_s^{k-1} \left( 1 + \frac{N}{2\pi} \Delta\beta \right) \tag{26}$$

If  $\Delta\beta$  can be obtained in real time, the relationship between sampling and modulating frequency can be adjusted. Therefore  $f_s = Nf_c^k$  is an identical relation [12], and the influence of the spectrum leakage can be eliminated.

According to the above analysis, we propose a self-adaptive tracking method. In the method, we use a sinusoidal-signal generator, a pulse generator, and self-adaptive

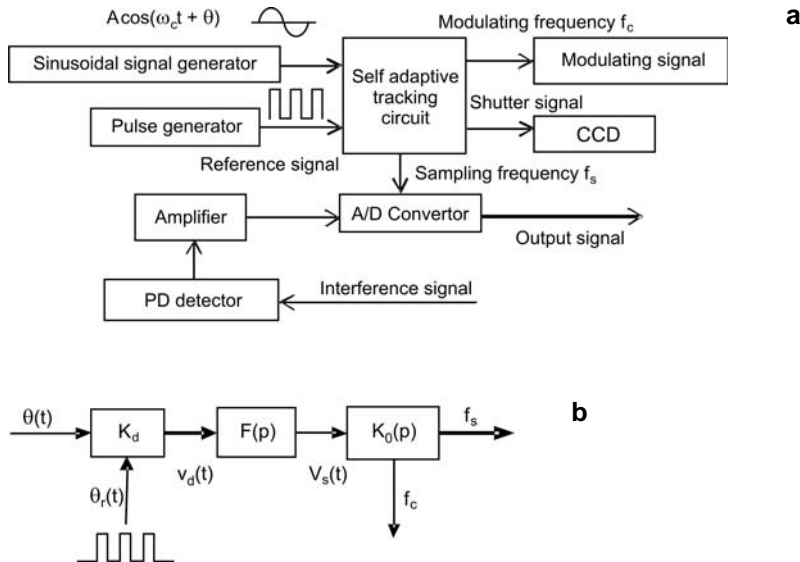


Fig. 2. Schematic diagram of the setup of self-adaptive tracking method (a) and the model of the self-adaptive tracking circuit (b).

tracking circuit (containing a frequency demultiplier), shown in Fig. 2a. The pulse signal generated by a pulse generator is an input into the self-adaptive circuit with sinusoidal modulation signal to operate in synchronism. Then the signals, including sinusoidal-modulated signal ( $f_c$ ), sampling signal of A/D conversion ( $f_s$ ), and shutter signal controlling CCD, are generated in synchronism. Therefore, the modulation and sampling signals work in synchronism, which can eliminate the frequency leaking. The self-adaptive tracking circuit is shown in Fig. 2b, and the operation process is as follows.

The output voltage  $V_s(t)$  changes with the phase difference which arises from the phase comparison between the sampling and reference signal shown in Fig. 2a. The voltage is converted into the signal varying with the frequency. After frequency division, the signal can be used to track and control the frequency of the modulating signal. The modulating signal varies with the sampling signal, and they keep determined integer multiple relations. The application model of the self-adaptive tracking method is shown in Fig. 2b.

The key point in the tracking method is to obtain the phase difference  $\Delta\beta$  between the  $k$ -th and  $(k-1)$ -th window, and the real time adjust of the relationship between  $f_c$  and  $f_s$ . The phase of the sampling signal is  $\theta(t)$ , and the phase of the reference signal generated by oscillator is  $\theta_r(t)$ . According to the model, we have

$$\Delta\beta = \theta(t) - \theta_r(t) \quad (27)$$

transformed by the phase demodulator,  $\Delta\beta$  is converted into voltage, and

$$v_d(t) = K_d \cos(\Delta\beta) \quad (28)$$

where  $K_d$  is the gain. After low-pass filter,  $v_d(t)$  is transformed into  $v_c(t)$

$$v_c(t) = F(p)v_d(t) \quad (29)$$

where  $p$  is an operator, and  $F(p)$  is the operator of the linear differential equation. The modulating frequency  $f_c(t)$  is generated by the operator  $k_0/p$ , and is given by

$$f_c(t) = \frac{K_0}{p} v_s(t) \quad (30)$$

In Figure 3, after  $k$  frequency division,  $f_c$  is converted into the sampling frequency  $f_s(t)$ . The  $f_s$  and  $f_c$  are controlled by  $k_0(p)$ , and the relationship between  $f_s$  and  $f_c$  is given by

$$f_s = kf_c \quad (31)$$

Equation (31) is the identity equation. Therefore the spectrum leakage is eliminated and the system stability is enhanced.

## 7. Simulation and experimental results with the new method

In this section, simulation and experimental results with the new self-adaptive tracking method are presented. The theoretical value of the surface profile is 100 nm, SNR 50 dB, light wavelength 632.8 nm, real sampling frequency is as that shown in Tab. 2, ideal sampling signal frequency is 3200 Hz, and the number of sampling points  $N$  is 128. According to Eqs. (2)–(4) and Eqs. (30)–(31), we get the discrete interferometer signal. After the Fourier transform to the discrete signal, the  $n$ -th ( $n = 1, 2, 3$ ) order spectrum component ( $S_1$ – $S_3$ ) without frequency leakage can be obtained when  $\delta(\Delta\omega) = 1$ , and the simulated surface profile  $r(x, y)$  can be calculated from Eqs. (10)–(12) and Eqs. (13)–(14). The simulated results of the self-adaptive tracking method are shown in Tab. 2. The spectrum leakage errors, without and with corrections shown in Tabs. 1 and 2, respectively, are presented in Fig. 3.

In the experiment, experimental setups shown in Figs. 1 and 2 are used, and the measured object is an optical wedge. A point in the wedge whose surface profile is about 100 nm is chosen. In the measurement experiment, the light wavelength is 632.8 nm, real sampling frequency is as that shown in Tabs. 1 and 2, ideal

T a b l e 2. The errors of the simulated spectrum leakage corrected by the self-adaptive tracking method.

Modulating frequency [Hz]	Real sampling frequency [Hz]	Average displacement [nm]	Repeatable accuracy [nm]	Error [nm]
401.5	3212	100.15	1.96	0.15
401.35	3210.8	100.31	1.96	0.31
401.2	3209.6	100.16	1.96	0.16
401.05	3208.4	100.33	1.97	0.33
400.925	3207.2	100.31	1.96	0.31
400.75	3206.0	100.08	1.96	0.08
400.6	3204.8	100.12	1.67	0.12
400.45	3203.6	100.32	1.97	0.32
400.25	3202.0	100.31	1.96	0.31
400.15	3201.2	100.15	1.97	0.15
400	3200	100.16	1.98	0.16
399.85	3198.8	100.32	1.97	0.32
399.7	3197.6	100.32	1.97	0.32
399.55	3196.4	100.31	1.96	0.31
399.4	3195.2	100.15	1.98	0.15
399.25	3194.0	100.32	1.96	0.32
399.1	3192.8	100.32	1.98	0.32
398.95	3191.6	100.33	1.96	0.33
398.8	3190.4	100.31	1.96	0.31
398.65	3189.2	100.33	1.98	0.33
398.5	3188.0	100.16	1.96	0.16

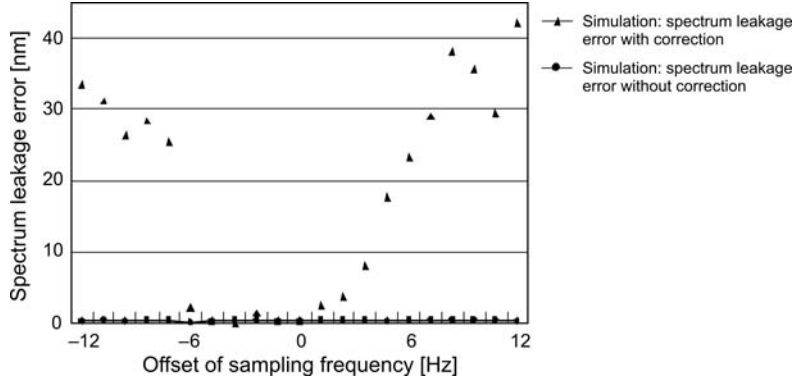


Fig. 3. The simulation spectrum leakage errors with and without correction.

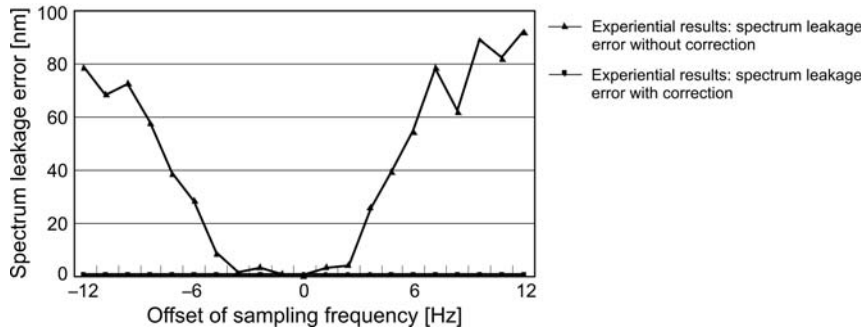


Fig. 4. The experimental spectrum leakage errors with and without correction.

sampling signal frequency is 3200 Hz, and the number of sampling points  $N$  is 128. The experimental results with and without the self-adaptive tracking method are shown in Fig. 4. In this figure, the spectrum leakage error without correction is larger than that in Fig. 3 due to the high level noise in the experiment.

The simulation and experimental results with the self-adaptive tracking method shown in Figs. 3 and 4 verify the correctness and validity of the tracking method. The simulation condition in Eq. (31) is satisfied. It is easy to see from Figs. 3 and 4 that the tracking method solves the problem of the spectrum leakage, decreases the measured displacement error, and increases the repeatable accuracy. Therefore, the self-adaptive tracking method can enhance the measurement accuracy greatly. The measured result need not to be amended, which can shorten the time of data processing.

## 8. Conclusions

In this paper, we theoretically analyze the accuracy in the surface profile measurement in the sinusoidal phase modulating interferometer, derive the relative error formula, analyze quantitatively the relative error of the  $k$ -th ( $k = 1, 2, 3$ ) order spectrum, and

simulate the influence of spectral leakage on measurement accuracy. The theoretical results show that the spectrum leakage introduces the absolute error which is higher than  $\lambda/320$  nm. When the offset of sampling frequency is in the range of  $-0.188\%$  to  $+0.075\%$ , the spectral leakage is negligible. In order to eliminate the influence of the spectral leakage, a self-adaptive tracking method is proposed. According to the fluctuation of the sampling signal frequency, the tracking method can adjust automatically the sampling signal frequency in such a way that the sampling signal frequency is an integer multiple of the modulating signal frequency. The simulation and experimental results show that this technique can solve the problem of the spectrum leakage, and enhance the measurement accuracy and system stability of the SPM interferometer. It can be used in the field of displacement, surface profile, and vibration measurement.

*Acknowledgments* – It is gratefully noted that the work was supported by the National Natural Science Foundation of China under Grant No. 60607007 and 60674097, and Natural Science Foundation of Chongqing Normal University under Grant No. 08XLB006.

## References

- [1] OSAMI SASAKI, HIROKAZU OKAZAKI, *Sinusoidal phase modulating interferometry for surface profile measurement*, Applied Optics **25**(18), 1986, pp. 3137–3140.
- [2] XIANGZHAO WANG, OSAMI SASAKI, TAKAMASA SUZUKI, TAKEO MARUYAMA, *Measurement of spatially nonuniform phase changes of a light beam utilizing the reflectivity characteristic of the self-pumped phase-conjugate mirror*, Optical Engineering **38**(9), 1999, pp. 1553–1559.
- [3] TAKAMASA SUZUKI, TAKAO OHIZUMI, TATSUHIKO SEKIMOTO, OSAMI SASAKI, *Disturbance-free distributed Bragg reflector laser-diode interferometer with a double sinusoidal phase-modulating technique for measurement of absolute distance*, Applied Optics **43**(23), 2004, pp. 4482–4487.
- [4] TAKAMASA SUZUKI, HIROMI SUDA, OSAMI SASAKI, *Double sinusoidal phase-modulating distributed-Bragg-reflector laser-diode interferometer for distance measurement*, Applied Optics **42**(1), 2003, pp. 60–66.
- [5] XUEFENG ZHAO, TAKAMASA SUZUKI, TAKAMASA MASUTOMI, OSAMI SASAKI, *Sinusoidal phase modulating laser diode interferometer for on-machine surface profile measurement*, Optical Engineering **44**(12), 2005, p. 125602.
- [6] YANDE XU, *Two-period interference fringes interferometry*, Optical Engineering **44**(4), 2005, p. 045601.
- [7] LI DAILIN, WANG XIANGZHAO, WANG XUEFENG, *et al.*, *Composite light source interferometer for real-time micro vibration measurement*, Chinese Journal of Lasers **31**(3), 2004, pp. 350–353.
- [8] TAKAMASA SUZUKI, XUEFENG ZHAO, OSAMI SASAKI, *Phase-locked phase-shifting laser diode interferometer with photothermal modulation*, Applied Optics **40**(13), 2001, pp. 2126–2131.
- [9] ZHANG CAINI, WANG XIANGZHAO, *High-accuracy angular displacement measurement using sinusoidal phase-modulating Fabry–Perot interferometer*, Acta Optica Sinica **24**(8), 2004, pp. 1141–1145.
- [10] WANG MAOHAI, LIU HUIJIN, PENG HUI, ZHANG GUOQIANG, *Analysis on errors of discrete fourier transform (DFT) in case of signal frequency drifting from designed value*, Electrical Measurement and Instrumentation **38**(421), 2001, pp. 13–16.
- [11] YOUHENG XU, BAOPING JU, *Synchronized phasor measuring method using recursive DFT with a window function*, Transmission and Distribution Conference and Exhibition: Asia and Pacific, IEEE/PES, 2005, pp. 1–6.
- [12] LIU JINMING, YING HUAIQIAO, *The dominant frequency position's influence on FFT spectrum leakage*, International Conference on Signal Processing Proceedings, ICSP, Vol. 1, 1996, pp. 241–245.

- [13] HARRIS F.J., *On the use of window for harmonic analysis with discrete Fourier transform*, Proceedings of the IEEE **66**(1), 1978, pp. 51–83.
- [14] OSAMI SASAKI, KAZUHIDE TAKAHASHI, *Sinusoidal phase modulating interferometer using optical fibers displacement measurement*, Applied Optics **27**(19), 1988, pp. 4139–4142.
- [15] TAKAMASA SUZUKI, TAKAYA MUTO, OSAMI SASAKI, TAKEO MARUYAMA, *Wavelength-multiplexed phase-locked laser diode interferometer using a phase-shifting technique*, Applied Optics **36**(25), 1997, pp. 6196–6201.
- [16] MA RENZHENG, CHEN MINGKAI, *An adaptive sampling tracking method for reducing spectrum leakage*, Automation of Electric Power Systems **4**(10), 2002, pp. 55–58 (in Chinese).
- [17] OSAMI SASAKI, HIROKAZU OKAZAKI, *Analysis of measurement accuracy in sinusoidal phase modulating interferometry*, Applied Optics **25**(18), 1986, pp. 3152–3158.

*Received September 18, 2007  
in revised form August 9, 2008*